Development of a Mathematical Framework to Describe Nerve Regeneration in Implantable Conduits

CoMPLEX MRes Mini-Project 1, May 8, 2014

Author:

Talfan Evans

Supervisors:

Dr. James Phillips and Dr. Rebecca Shipley

Abstract

This study provides a review, and an investigation into the design of Nerve Guidance Conduits for the purpose of peripheral nerve regeneration. Analysis of their post-construction stability is conducted, with a view to experimenting with further geomtries. A computational model is also presented, investigating a range of NGC geometries and the effect of physiological biases guiding growth.

Contents

1 Introduction

Peripheral nerve injuries currently affect more than 1 million people worldwide, with more than 300,000 cases reported each year in the US alone, though the severity of these injuries varies dramtically. Neuropraxia and axonotmesis are characterised by a disruption in the function of the nerve cell axon, commonly attributed to crushing and contusion injuries, however whereas these injuries have in general a good prognosis, neurotmesis describes a more severe degree of damage. Here, transection, burns and degenerative disorders all contribute[8, 7] to the complete or partial severance of the axon and its encapsulating myelin sheath, often leading to permanent and debilitating loss of function. Where nervous regeneration is not completely successful, neuromas may form, benign growths of undirected neuronal growths which are often followed by neuropathic pain of which relief is only observed in 40-60% of cases[25].

Though spontaneous regeneration may occur over small gaps, functional restoration is often poor, and microsurgical repair is preferred[9]. This approach is however limited to tension-free suturing of the proximal and disal ends, and in practice is only effective at distances of approximately 5mm[10]. Beyond these distances, recovery rates are poor, with the "gold standard"[6] autograft repair typically demonstrating a 50% success.

This has remained the case for approximately 50 years, with little new successful innovations introduced, in spite of the several downsides associated with autografts, largely associated with the difficulty of surgical implementation. Grafts must be transplanted from an external site on the host and so are not only limited in supply but add additional complexity to the surgical procedure, and may introduce other problems including donor site morbidity, neuroma formation and scarring.

Allografts perform an identical function, and are preferred at gaps greater than 5cm due to their superior availability from external donors. This however introduces many more significant problems, with extensive immune suppression required for up to 18 months following implantation to prevent chronic inflammation and pain.

The state of these current techniques, in addition to the birth of tissue engineering as a field in its own right, has prompted renewed efforts towards addressing these issues, specifically in the field of articial implantations. Research has focussed primarily on the development of Nerve Guidance Conduits (NGCs),

typically hollow tubes of biocompatible materials, designed to ensheath and direct nerve regeneration.

As synthetically produced devices, they suffer few of the impracticalities associated with the removal and reimplantation of biological tissue. Although current versions do not currently offer comparable in vivo performance to autografts and are limited to gaps of 3-4cm[6], rapid advancement in the understanding of cell proliferation, material technologies and bio-integration offer profound potential improvement.

1.1 Scope of current technology

To better understand current design approaches, it is important to understand the process of peripheral nerve regeneration. Initially, both the distal and proximal nerve stumps exude neurotrophic factors and extracellular matrix (ECM) precursor molecules. Among these molecules is fibrinogen, which within the established favourable growth medium forms predominantly acellular fibrin cables throughout the volume which, whilst not performing any nervous function form a preliminary bridge between the two ends.

Schwann cells produced at proximal and distal stumps, along with endothelial cells and fibroblasts are able to migrate along these cables, aligning and forming the glial bands of Büngner. Trophic gradients also act to direct this growth[12], also secreted by the proliferating Schwann cells.

During the axonal phase, new regnerative axonal sprouts follow these bands, forming neuromuscular junctions after meeting the distal stump. At this stage, the Schwann cells change to a myelinating phenotype, encasing the larger axons in a myelin sheath, fully restoring function to the nerve. In experiments conducted by Williams et al.[27] in a 10mm rat sciatic nerve (RSN), the process is observed to occur over a period of 2-4 weeks.

Development has thus focussed on two primary areas, the first being the directing of neurite growth through the inclusion of structure within the NGCs. Matsumoto et al. [15] attempted to introduce such intraluminal guidance by introducing longitudinally arranged, laminin-coated collagen fibres. This concept was explored further by Yoshii et al.[16], who used these fibres without the NGC in RSN trials. Although neither demonstrated significant functional restoration over hollow conduits, 20-30mm gaps were succesfully bridged, improving significantly on the 15mm limit obtained in previous efforts.

Ngo et al.[18] initiated an invesigation into the internal architecture, showing high packing densities to be potentially inhibitory to growth, a finding echoes by Stang et al.[28] in conduits packed with a dense

collagen sponge.

Hadlock et al. attempted to mimi more closely the microstructure of the ECM, using a foam-processing technique to produce micro channels within a PLGA conduit[19], demonstrating reduced axonal dispersion.

The second focus has been on the seeding of autologous or allogenic SCs within the NGCs, where cells can be cultured in vitro to form pre-established scaffolds that reduce the uncertainty associated with preliminary bridging after implantation. Schwann cells encourage myelination of the the regenerating neurites[20], and along with preintroduced growth factors NGF[23] and BDNF[24] at an optimum concentration have been demonstrated to double the rate[21] of regeneration compared with hollow acelullar NGCs.

1.2 Outline of investigation

Despite these efforts, data describing the performance of the various architectures is sparse, as the construction and clinical evaluation of NGCs is an inherently expensive and time-consuming process. Large-scale, undirected experimentation is therefore impractical, with existing studies focussing mainly on comparatively simply produced geometries.

It is here that computational modelling can play an important role. Though the complexities of biological systems are difficult to capture in exact detail, their aggregate behaviours are nevertheless often reproducible, especially when reinforced with accurate experimentally obtained parameters. Applied in this instance, a computational model of neurite growth can thus act as a useful initial comparison between the myriad geometrical configurations constructuctable, and so guide the direction of future clinical investigation. However, much work also remains from a clinical standpoint, with specific regard to the contruction of these conduits, as little is known about their subsequent in vivo stability.

This investigation aims therefore to attack the problem both from a clinical and computational perspective. The first section details examinations into the post-construction microstructure of a variety of collagen-based NGCs, following previous work by Girorgiou et al.[5], with an aim to determining the in vivo validity of their approach. The second section describes the development of a computational model to simulate neurite growth in a selection of designed geometries, to investigate their effectiveness in facilitating this growth.

2 Collagen conduits

Though tissue engineering employs a range of polymers, ceramics and other synthetically produced materials, their benefits are most often conferred in terms of strength and durability, and as such are well suited to the construction of load bearing structures. However, their often limited immunogenic properties make them an impractical choice where sensitive integration with cells are concerned, and for these purposes, naturally derived tissues such as collagens are often preferred, though immunogenicity is only one aspect of overall biocompatibility of materials. Cells are known to be extremly sensitive to the mechanical propeties of tissue[1], and it is this ability to interact with cells that make natural materials a favourable choice.

Collagen as a biomolecule and biomaterial has been studied extensively, owing to its ubiquity among the connective tissues of the body. Comprising approximately 25% of the total dry weight of mammals[3], fibrous collagens form the bulk of the extracellular matrix (ECM), the multicellular scaffold providing biochemical and structural support to cells in vivo.

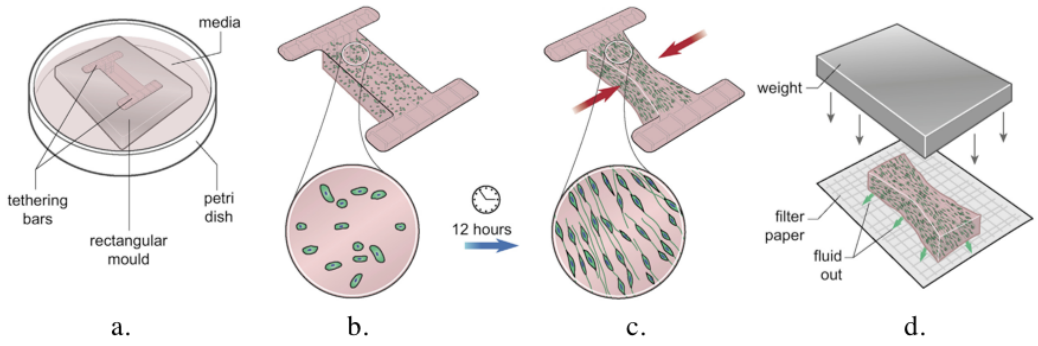

Figure 1: Outline of aligned EngNT construction, reproduced from Giorgiou et al.[5]

Type I collagen is a particularly popular choice for tissue engineering applications, being easily available and highly versatile[2] in addition to possessing the aforementioned biocompatible properties. In particular, its fibrous structure makes it amenable to alignment in response to force vectors, resulting in an anisotropicity that has been found to be critical to, among other biological instances, the self alignment of cells seeded within the material. In the case of the clinical repair of peripheral nerve injuries, neurite

growth has been found to be highly sensitive to Schwann cell alignment, an absence of which typically leads to scarring and poor restoration of mechanical function[**?**, **?**].

However, collagen in its fully hydrated state exists as a hydrogel which does not maintain it's anisotropic state when force vectors are removed, diminishing its potential for usage in vivo. However this investigation follows promising work done by Giorgiou et al.[5], who have developed a simple and effective method of stabilising these engineered tissues (EngNT) using plastic compression techniques, outlined in fig. 1.

Firstly, the collagen gel, seeded with a Schwann cell suspension, is incubated within a tethering mould. During the incubation, the cells contract and elongate along the longitudinal axis before plastic compression using a weighted absorber is applied, rapidly removing the fluid from the hydrogel. Careful removal of the absorber results in a stable, robust sheet of tissue-like material, preserving cellular alignment without the use of cross-linking agents, which can inhibit successful integration with the host cells[5].

2.1 Geometry justification

The resulting sheets are typically 40-60ţm in thickness, and can be used to form the final geometry of the nerve conduits. Preliminary work has focused on rolling the sheets into rod type architectures, due both to their comparative ease of construction and structural stability. These rods are then encased within a Neurawrap tube to form the final implantable device.

In an 8 week growth experiment[5] conducted in a 15mm gap rat sciatic nerve model, neurite growth was found to be subtantially superior when compared to an empty tube containing no collagen rods. Of those neurites that succesfully succesfully reached the proximal conduit from the proximal stump, approximately 70% were succesfully directed towards the distal end. However only approximately half as many neurites succesfully spanned this gap in comparison to the nerve autograft, suggesting that the bottleneck in the performance of the device may lie in facilitating this initial entry and prompting further investigation.

2.2 Flat-cut vs. roll-cut

It has been hypothesized that, whilst structurally stable, the exposed ends of the collagen rods might be vulnerable to deformation both during the construction process and when subsequently implanted, which could potentially act to impede the entry of neurites at the proximal end.

During their construction, the rods are typically rolled by hand and cut (roll-cut) to produce two rods of equal length. To assess the impact of this process, a second sample was prepared for comparison, cut before rolling (flat-cut). The ends of each sample were examined using SEM, illustrated in fig.2.

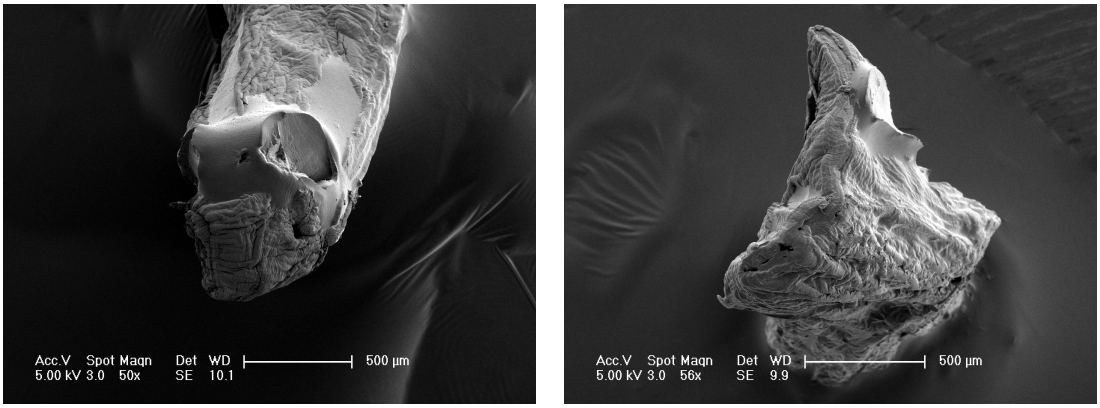

(a) A flat-cut end

(b) A roll-cut end

Figure 2: End-comparison, smooth gel

In order to image the samples, they were first fixed in gluteraldehyde over a one-week period, dehydrated and sputter-coated with a gold/palladium alloy. Before proceeding, it is noted that although the fixing process aims to form reinforcing cross-linkages between the collagen fibres, the hydrogel's high water composition resulted in significant contraction during the dehydration process, in some cases obscuring it's structure. This would not however be the case in vivo, where the gels would be immersed in a fluid medium.

Fig. 2a shows firstly the effect of the dehyrdation process, clearly exaggerating the contraction. However, the contrast between this and fig.2b, illustrating the sample cut whilst rolled is significant. The roll-cut

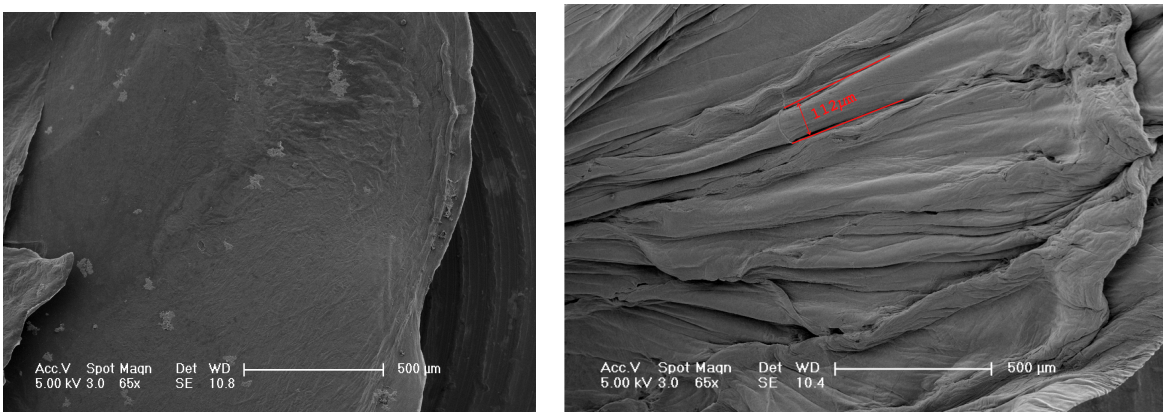

(a) Smooth (b) Ridged

Figure 3: Comparative microstructure of gels

sample shows clear evidence of compression during the cutting process, acting to crimp the ends together, effectively sealing the entry. No such symptoms exist in the flat-cut sample.

2.3 Ridged vs. smooth, flat sheet

In a similar vein to the work by [19], a novel architecture was proposed to introduce integrated micro channels into the structure of the gels so as to avoid the possibility of growth inhibition due to the density of the packing[28]. To achieve this, an absorber with a ridged surface was used during the compression phase (fig. 1d), which can then be rolled in a similar fashion with ridges aligned longitudinally.

Fig. 3 shows the comparative microstructure of two flat sheets of compressed gel. The ridges, where absent in the sample produced using a smooth-faced absorber (fig. 3a) are clearly visible in the ridged sample (fig. 3b).

Moreover, the ridges can be seen to be of order ˜100ţm in width, providing sufficient space for neurites, typically 5-10ţm in diameter to grow.

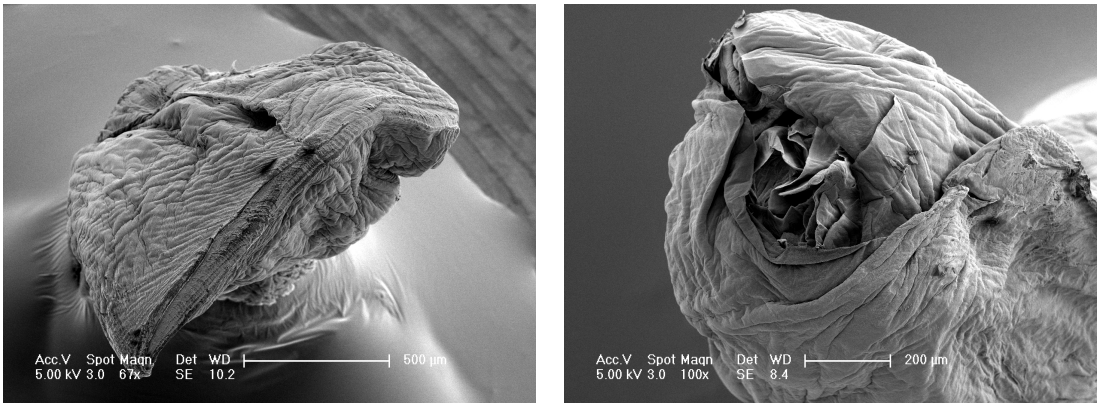

(a) A roll-cut end, ridged gel

(b) A flat-cut end, ridged gel

Figure 4: End-comparison, ridged gel

2.4 Ridged vs. smooth, cut ends

Though present in the compressed sheets, it is unclear whether this structure would be preserved following the rolling process. Fig. 4 shows a comparison of the roll-cut and flat-cut ends.

Unlike in fig. 2, the internal structure of the flat-cut end is clearly visible, displaying a clear concentric arangement with well established entry points for neurite growth. The effect of the roll-cutting processing is again emphasized in fig. 4a, showing again the crimping effect observed in the smooth sample.

Neither image shows clear evidence of the embedded micro channels clearly visible in the unrolled sheet, suggesting their structure to be unstable, and susceptible to collapse when manipulated. It is possible however that the dehydration process played a contributory role, as the concentric layers would likely flatten in contraction.

2.5 Extruded shapes

A further point of interest to the future development of the NGCs is whether they are amenable to forming more complex, longitudinally varying 3D structures. Though it is yet to be verified as to whether such structures would confer any performanec improvements, one hypothesis follows that during initial regener-

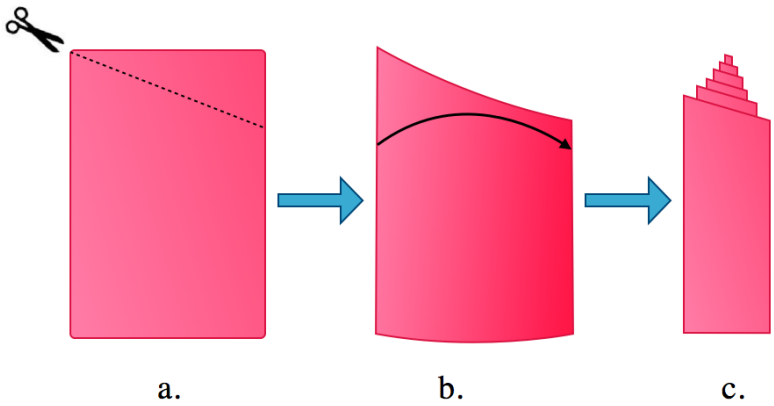

Figure 5: Constructing the extruded geometry

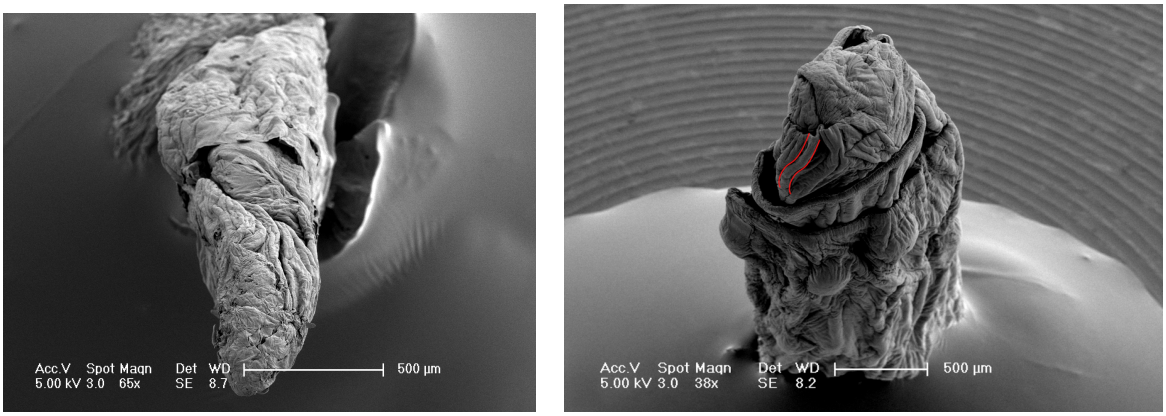

(a) Smooth

(b) Ridged

Figure 6: Extruded ends

ation, neurites might benefit from receiving an increasing level of scaffold as they progress longitudinally, so as not to impede initial growth at the nerve stumps.

A simple cone-type geometry was therefore simply constructed by making an angled cut in the flat sheet before rolling, as illustrated in fig. 5. Fig. 6 demonstrates that in both the smooth and ridged gels, a clear extruded structure is present, suggesting that the gel could maintain such an arrangement in vivo.

Importantly, fig. 6b shows evidence of preserved ridged structure conforming to the expected dimensions

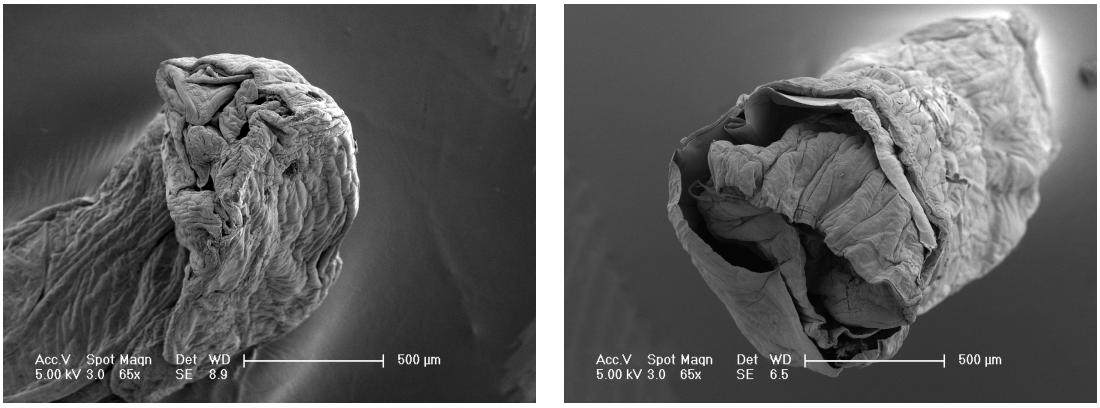

(a) Smooth (b) Ridged

Figure 7: Intruded ends

$\sim O(100\mu m)$, whereas the smooth gel (fig. 6a) shows none. The inverse geometry can also be easily constructed by reversing the order of rolling, creating an intruded spiral structure, however the nature of this configuration gives it an inherent susceptibility to end collapse, especially when aggravated by the dehydration process. Though the smooth gel (fig. 7a) is seen to exhibit this, the ridged gel (7b) displays remarkably clear evidence of retreating concentric layers as intended. It is noted that this is more likely to be attributed to variability in the SEM preparation than to differing structural properties between smooth and ridged gels.

3 Model

Regenerating neurites respond to a variety of environmental cues. In the most fundamental case, one neurite may physically impede the growth of another by occupying space, especially where micro-channels engineered into the conduit, or limited surface area is concerned. Whilst it has been demonstrated [5] that neurites respond to alignment in pre-seeded Schwann cells, proliferating Schwann cells also release trophic factors which may lead to self-alignment. Where an existing trophic field exists, metabolic uptake upstream may cause subsequent neurites to recieve altered trophic signals, prompting time and space dependent growth paths.

For these reasons, it is not physiologically realistic to model neurite growth on an individual basis, and simulations must be conducted in fully parallel fashion. In this case, and as is often the case where biological systems are concerned, deterministic modelling approaches are unfeasible, due both to scale of the task and to the inherent stochasticity associated with the growth of individual neurites.

3.1 Stochastic modelling and the Gillespie algorithm

The stochasticity of the neurite growth is implemented using the Gillespie Algorithm[29], a discrete-event simulation algorithm which, unlike other stochastic simulation algorithms, simulates each reaction event and can be shown to generate an exact realisation of the underlying model.

Here, each 'event' may refer either to the sprouting of a new neurite in the distal stump, or to the growth of an existing neurite in $n \in N$ in a particular direction. To simulate as a discrete process, the growth and sprouting rates are converted into reaction hazards h_g and h_{sp}, representing the probability of an event occurring within any given time interval Δt. The total time to the next reaction is calaculated as a function of the total hazard h_0 of all possible events.

The domain of the conduit is also discretised with a grid spacing $L\,(\frac{mm}{voxel})$, such that the neurite can grow in one of six directions $X_0^{t+\Delta t} \rightarrow \{z+1, z-1, x+1, x-1, y+1, y-1\}$, where z is the longitudinal and x and y the radial directions.

Neurites are sprouted at the proximal stump at $z = 0$, within the proximal space S, and progress into the conduit C. The proximal space must exist so as to prevent the conduit from touching the proximal

stump, and so possibly hindering the sprouting of new neurites. Upon contact with the conduit material, a neurite will exerience a growth bias h_s in either longitudinal direction perpendicular to the material based on the presence of aligned Schwann cells, such that the neurites are encouraged to adhere to the surface, using the NGC as a growth scaffold.

A constant longitudinal bias h_c is also present throughout the conduit and proximal space, encouraging positive longitudinal growth so as to simulate a trophic gradient. Lastly, the proximal space is bounded, and a neurite may not grow into any position in the conduit space in which any neurite has previously grown. The algorithm thus can be summarised as follows:

1. Characterise the system at $t = T$ by calculating the hazard of growth in each direction for every neurite $n \in N$.
2. Simulate the time to next reaction event $\Delta t \sim Exp\,(h_0)$.
3. Select an event at random, based on it's weighted hazard $\frac{h_i}{h_0}$.
4. Update the system with the new position of the current neurite n.

The sprouting hazard is calculated to correspond to the approximately 5000 neurites generated in experimental observations over a period of 14 days, and the neurite growth rate as approximately $1\frac{mm}{day}$. Experiments evidence (fig. 3b, Giorgiou et al.[5]) suggests that neurites align highly preferentially to the orientation of Schwann cells. However, in lieu of a rigorous quantitative study, the sheet and chemotactic biases are set modestly to $h_s = h_c = 3 \times h_g$.

3.2 Description of geometries

3.2.1 Spirals

A regular Archimedean spiral with origin at $r = 0$ is represented on a polar axis by the equation $\zeta = \beta\theta$, where ζ is the non-dimensional radius from the centre, θ the angle and β the spacing coefficient, where the number of turns is given as $N = \frac{1}{2\pi\beta}$. The surface area is twice the sheet length, where neurites are able to

Parameter	Symbol	Value
Grid Spacing	L	0.01mm/voxel
Simulation Duration	T	14 days
Radius of Conduit	R	1mm
Unbiased Neurite Growth Hazard	h_g	$0.00116s^{-1}$
Sheet Bias	h_s	$0.00348s^{-1}$
Chemoattractant Bias	h_c	$0.00348s^{-1}$
Sprouting Hazard	h_{sp}	$0.0041s^{-1}$
Proximal Space Length	S	0.02mm

Table 1: Simulation Parameters

(a) $\eta \propto \frac{1}{w}$ (b) Intermediate η and A_s (c) $A_S \propto N$

Figure 8: Varying η and A_S for spiral geometries

adhere to both sides of the surface, and is thus independent of the sheet thickness ω, non-dimensionalised by the conduit radius R, given as:

$$\phi_S = \frac{1}{\beta} \tag{1}$$

However, the porosity η is dependent on both the thickness and the number of turns as :

$$\eta = \frac{\omega}{\beta} \tag{2}$$

Thus, it is possible to easily manipulate the surface area and porosity of the geometry independently, as seen in fig. 8.

3.2.2 Horizontal sheets

(a) $\eta \propto \frac{1}{w}$ (b) Intermediate η and A_s (c) $A_S \propto N$

Figure 9: Varying η and A_S for stacked sheet structures

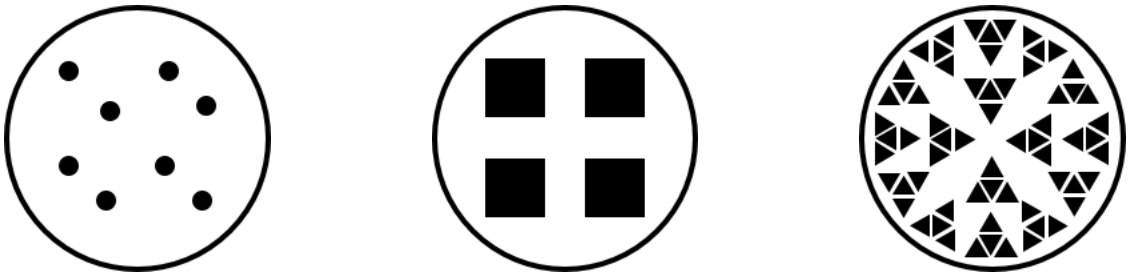

(a) $\eta \propto \frac{1}{Nd^2}$ (b) Intermediate η and A_s (c) $A_S \propto Nd$

Figure 10: Varying η and A_S for stacked sheet structures

3.2.3 Rods

3.3 Towards experimental and computational integration

To durther investigate the post-construction structure of the NGCs, 10ţm cross-sections were taken in a cryostat, the collagen stained using Toluidine blue and imaged using an optical microscope. The results, shown in fig. 11 show clear concentric structure with space preserved between succesive layers.

For future experiments, it is desirble to be able to compare the performance of idealised, digitally constructed geomtries to the those obtained in practice. To this end, it was possible to input the cross-sectional images into the simulator, following processing of the images into a suitable format, illustrated in fig. 12.

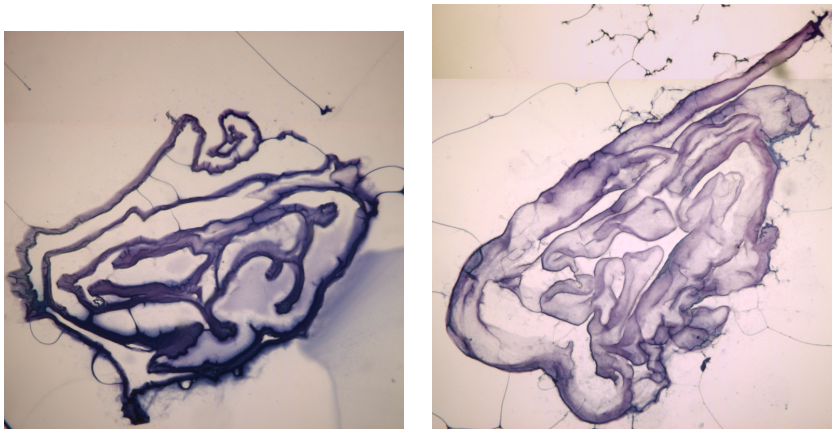

(a) Smooth section (b) Ridged section

Figure 11: Cross-sections of constructed spiral geometries, 10x lens

Figure 12: Re-formatted smooth spiral section

4 Simulation results

In the following section, the hit ratio is defined as the proportion of neurites that during their maximal longitudial progression exceed a prescribed distance. A hit ratio distance of $Z = 2mm$ was chosen as the a distance with which to compare growths. The average velocity of the neurites is defined as the final longitudianl position, divided by the time since sprouting.

4.1 Simulations in imported cross-section

Fig. 13a shows the effect of distance along the conduit on the hit ratio in the experimentally obtained cross-section. As expected, the hit ratio decreases with increasing distance, however surprisingly, the proportion of progressing neurites is low, with only 13% reaching a distance of 1mm into the conduit over 7 days. Upon closer examination, 13a shows that the average velocity of the neurites decreases rapidly with time, showing that whilst the growth velocity of the initial neurites is of the order of magnitude expected $\sim O\left(1mm/day\right)$, subsequent neurite experience little to no growth.

Upon inspection of the simulation data, it is observed that the initially sprouting neurites quickly occupy the proximal space, leaving subsequent neurite growths no space to fill. As such, the average hit ratios and velocities are reduced due to the proportion of the population experiencing no growth.

4.2 Horizontal sheets

Simulations on various horizontal sheet configurations again display low overall hit ratios. Fig. 14 shows firstly that, as expected, the hit ratio and average progression are proportional. Fig. 14a demonstrates firstly an increase in both hit ratio and V_{avg} with increasing surface area, followed by a sharp decrease after $A_s \approx 60$.

The initial increase is as expected, as an increased surface area would signify a greater proprtion intraluminal longitudinal bias. However, considering the geometry of the stacked sheet arrangement, the sharp decrease seems to suggest that, though the overall porosity remains constnt among the sections, directed random growth within small channels causes congestion, preventing further growth.

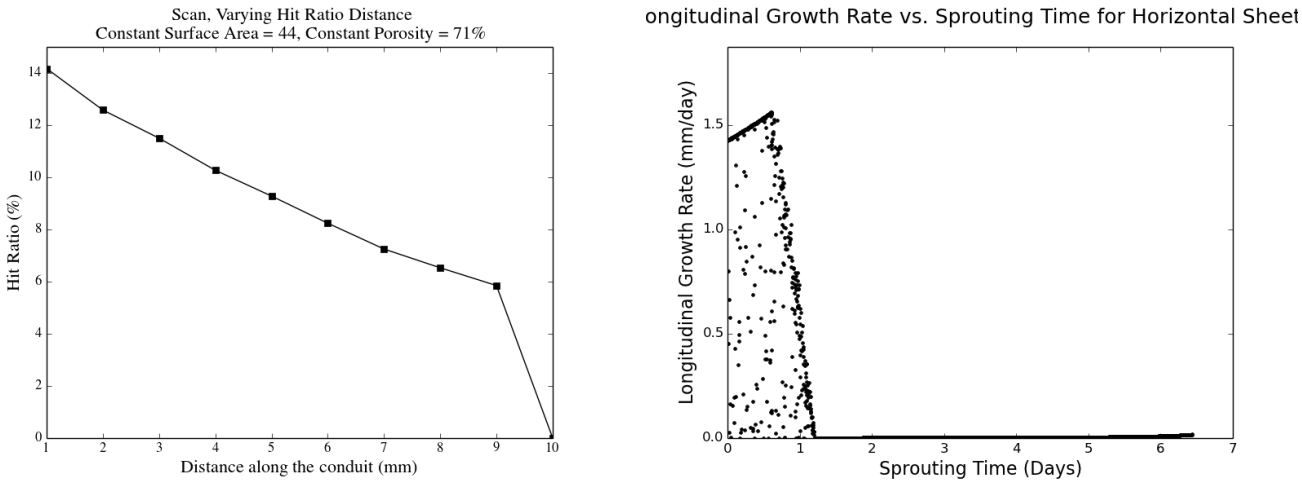

(a) Hit Ratio vs. Distance

(b) Average velocity vs. sprouting time

Figure 13: Simulations perfomred on scanned smooth spiral

Fig. 14b shows that a constant surface area, growth is highly sensitive to porosity, supporting the hypothesis that for this value of surface area, the benefits conferred by additional mechanical direction are counteracted by the impeding structure.

4.3 Spirals

Identical experiments conducted on spiral geometries yield similar results, displaying an equivalent increase in both hit ratio and V_{avg} with porosity. However, fig. 15a suggests that a further increase in surface area may act to counteract the congestion within channels where their width approaches that of the diameter of the neurites. In this case, growth would be completely directed, significantly reducing deviation from the longitudinal direction and preventing the behaviour observed at intermediate surface areas.

4.4 Rods

Fig. 16 shows simulations comparing longitudinal arrangements of circular, square and triangular rods. 16a show square rods to effect the greatest hit ratio, followed closely by the triangular sections. This is

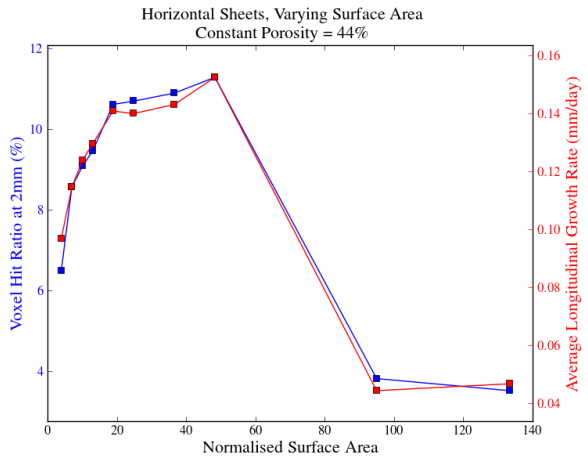

(a) Varying A_s

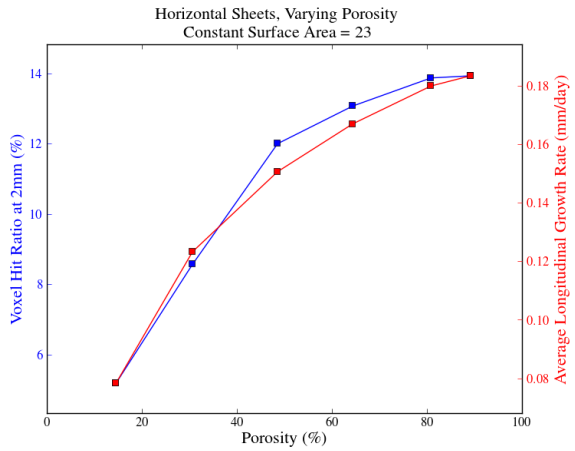

(b)

Figure 14

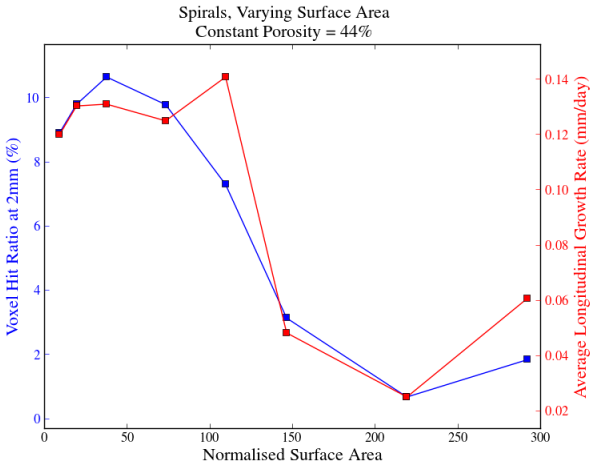

(a) VaryingA_s

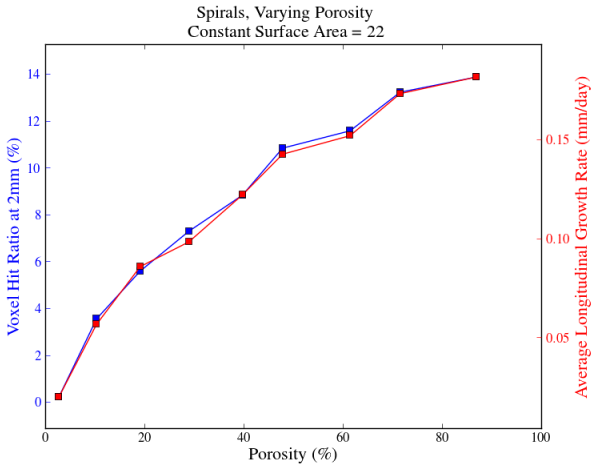

(b) Varying η

Figure 15

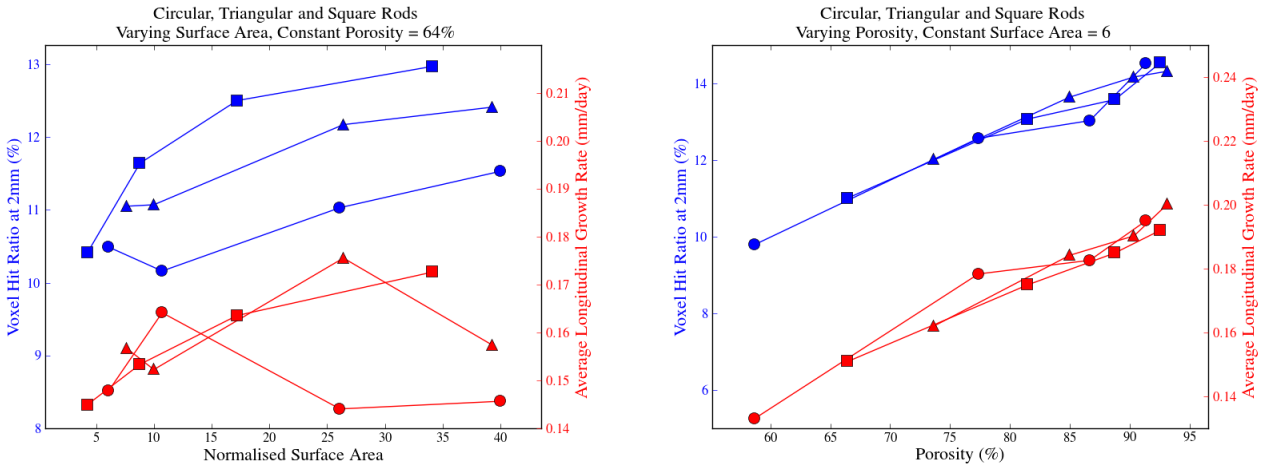

(a) VaryingA_s (b) Varying η

Figure 16

reflected in the V_{avg} simulations, where little separates the two. Surprisingly, the circular rods perform worse in both hit ratio and V_{avg}.

4.5 Varying growth biases

Fig. 17 shows the effect of varying the chemotactic and surface gradient respectively. As expected, there is a general increasing trend with increasing both. The experiments were conducted on a spiral of relatively high porosity, agreeing with the larger effect of chemotactic over surface bias, which directs neurite growth when not adhered to the NGC. However, 17a shows an initial spike in both hit ratio and V_{avg}, suggesting that there may be an optimal level.

5 Summary and further work

This investigation has demonstrated the potential of applying computational approaches to the design, evaluation and optimisation of NGCs. Section 2 investigated the post-construction stability of collagen-

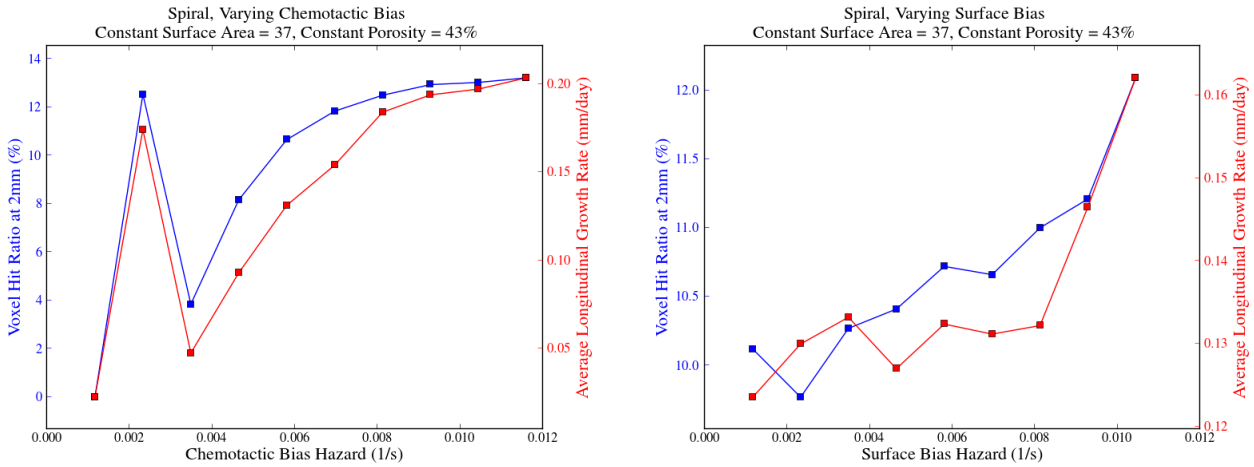

(a) Varying P_c

(b) Varying P_s

Figure 17: Varying bias hazards for a spiral geometry

based structures, where analysis of their entry points suggest that the low proportion of neurites making successful entry to the NGCs reported by [5] suggests that this may be due to a deformation of end structure firstly in construction, but also as a result of the delicate nature of the collagen sheets.

Attempts to optimize the end geometries were successful, showing that an extruded structure can be relatively easily accomplished, potentially providing a graduated entry to the NGC that could avoid the problem of collapse. Subsequent analysis of the cross-section of the geometries showed that the spiral structure is well preserved.

Finally, a novel construction technique was investigated for incorporating micro channels within the NGC using a ridged absorber. SEM analysis, though inconclusive shows some evidence of preserved ridged structure, though this was not evident in the cross-sections.

Section 4 concerned the development of a stochastic model for simulation of neurite regeneration in arbitrarily shaped conduits. The potential for interfacing experimental and computational approaches to conduit was emphasized by simulating growth in a scanned geometry. The model is in principle also capable of simulating growth in 3D, longitudinally varying conduits, though this was not enacted due to time constraints.

Simulations on a variety of geometries confirmed an initial dependence on both the surface and chemotactic biases affecting neurite growth. Comparisons of surface area at constant porosity yielded surprising results,

shown to increase performance in both hit ratio and V_{avg}, though past a particular limit, the advantage conferred may be counteracted by congestion in the increasingly small channels. Preliminary investigations into the effect of rod geometry show circles to perform inferiorily to squares and triangles, though further investigation is required to reinforce these findings.

Further simulations should be conducted at a higher grid resolution, which was not computationally feasible in the results shown. Though the resolution matched the diameter of the neurites, it was shown that space was quickly occupied in the proximal space, severely limiting subsequent growth.

References

[1] Stevens, M., George, J. H., 'Exploring and Engineering the Cell Surface Interface', (2005).

[2] 'Collagen-Based Biomaterials for Tissue Engineering Application', R. Parenteau-Bareil, R. Gauvin, F. Berthod.

[3] Alberts, B.; Johnson, A.; Lewis, J.; Raff, M.; Roberts, K., 'Molecular Biology of The Cell', Garland Science: New York, NY, USA, (2002).

[4] Brown R., Phillips J.B., 'Cell responses to biomimetic protein scaffolds used in tissue repair and engineering' (2007).

[5] 'Engineered neural tissue for peripheral nerve repair', Melanie Georgiou a, Stephen C.J. Bunting b, Heather A. Davies a, Alison J. Loughlin a, Jonathan P. Golding a, James B. Phillips .

[6] 'A biomaterials approach to peripheral nerve regeneration: bridging the peripheral nerve gap and enhancing functional recovery', W. Daly1, L. Yao1, D. Zeugolis1, A. Windebank2 and A. Pandit1

[7] Mukhatyar, V., Karumbaiah, L., Yeh, J. & Bellamkonda, R., 'Tissue engineering strategies designed to realize the endogenous regenerative potential of peripheral nerves', (2009)

[8] Siemionow, M. & Brzezicki, G., 'Current techniques and concepts in peripheral nerve repair', (2009).

[9] Jiang, X., Lim, S. H., Mao, H.-Q. & Chew, S. Y., 'Current applications and future perspectives of artificial nerve conduits', (2010).

[10] Belkas, S. J., Shoichet, S. M. & Midha, R. 2004, 'Peripheral nerve regeneration through guidance tubes'.

[11] Lee, S. K. & Wolfe, S. W., 2000 ,'Peripheral nerve injury and repair'.

[12] Lundborg, G. 2000, 'A 25-year perspective of peripheral nerve surgery: evolving neuroscientific concepts and clini- cal significance'.

[13] Chiono, V., Tondaturo, C. & Ciardelli, G. 2009, 'Artificial scaffolds for peripheral nerve reconstruction'.

[14] Kim, Y.-T., Haftel, V. K., Kumar, S. & Bellamkonda, R. V., 2008, 'The role of aligned polymer fiber based constructs in the bridging of long peripheral nerve gaps'.

[15] 36 Matsumoto, K., Ohnishi, K., Kiyotani, T., Sekine, T., Ueda, H., Nakamura, T., Endo, K. & Shimizu, Y. 2000, 'Peripheral nerve regeneration across an 80-mm gap bridged by a polyglycolic acid (PGA)-collagen tube filled with laminin-coated collagen fibers: a histological and elec- trophysiological evaluation of regenerated nerves'.

[16] Yoshii, S. & Oka, M. 2001, 'Collagen filaments as a scaf- fold for nerve regeneration'.

[17] Yoshii, S., Oka, M., Shima, M., Taniguchi, A. & Akagi, M. 2003, 'Bridging a 30-mm nerve defect using collagen filaments'.

[18] Ngo, T.-T. B., Waggoner, P. J., Romero, A. A., Nelson, K. D., Eberhart, R. C. & Smith, G. M. 2003, 'Poly(L-lactide) microfilaments enhance peripheral nerve regeneration across extended nerve lesions'.

[19] Hadlock, T., Sundback, C., Hunter, D., Cheney, M. & Vacanti, J. P. 2000, 'A polymer foam conduit seeded with Schwann cells promotes guided peripheral nerve regeneration'.

[20] 90 Mcgrath, A. M., Novikova, L. N., Novikov, L. N. & Wiberg, M. 2010, 'BDTM PuraMatrixTM peptide hydrogel seeded with Schwann cells for peripheral nerve regeneration'.

[21] Mosahebi, A., Woodward, B., Wiberg, M., Martin, R. & Terenghi, G. 2001, 'Retroviral labeling of Schwann cells: in vitro characterization and in vivo transplantation to improve peripheral nerve regeneration'.

[22] Di Summa, P. G., Kingham, P. J., Raffoul, W., Wiberg, M., Terenghi, G. & Kalbermatten, D. F. 2010, 'Adipose- derived stem cells enhance peripheral nerve regeneration'.

[23] X. Cao and M. S. Shoichet,'Defining the concentration gradient of nerve growth factor for guided neurite outgrowth'.

[24] J. Yamauchi, J. R. Chan, and E. M. Shooter, 2004, 'Neurotrophins regulate schwann cell migration by activating divergent signaling pathways dependent on rho gtpases'.

[25] R. H. Dworkin, A. B. O'Connor, and M. Backonja, 'Pharmacologic management of neuropathic pain: evidence based recommendation', 2007.

[26] Ijpma, F. F. A., Van De Graaf, R. C. & Meek, M. F. 2008, 'The early history of tubulation in nerve repair'.

[27] L. R Williams, F. M. Longo, H. C. Powell, G. Lundborg, and S. Varon, 'Spatial-temporal progress of peripheral nerve regeneration within a silicone chamber: parameters for a bioassay'.

[28] Stang, F., Fansa, H., Wolf, G., Reppin, M. & Keilhoff, G. 2005, 'Structural parameters of collagen nerve grafts influ-ence peripheral nerve regeneration'.

[29] Gillespie, D. T. (1976). 'A general method for numerically simulating the stochastic time evo- lution of coupled chemical reactions'.